NASA TECHNICAL NOTE

NASA TN D-2593

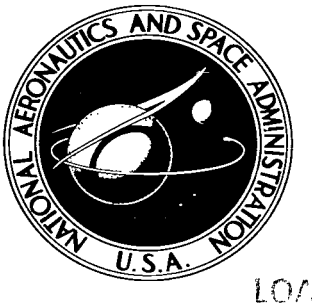

NASA TN D-2593

A FLIGHT INVESTIGATION OF THE SCOUT FOURTH-STAGE DIAPHRAGM SEPARATION DISTURBANCES

by Seymour Salmirs

Langley Research Center
Langley Station, Hampton, Va.

NATIONAL AERONAUTICS AND SPACE ADMINISTRATION • WASHINGTON, D. C. • FEBRUARY 1965

A FLIGHT INVESTIGATION OF THE SCOUT FOURTH-STAGE DIAPHRAGM SEPARATION DISTURBANCES

By Seymour Salmirs

Langley Research Center
Langley Station, Hampton, Va.

NATIONAL AERONAUTICS AND SPACE ADMINISTRATION

For sale by the Office of Technical Services, Department of Commerce,
Washington, D.C. 20230 -- Price $1.00

A FLIGHT INVESTIGATION OF THE SCOUT FOURTH-STAGE DIAPHRAGM SEPARATION DISTURBANCES

By Seymour Salmirs
Langley Research Center

SUMMARY

An investigation of the separation impulses of the Scout vehicle fourth-stage separation system was conducted during a flight of the ST-7 vehicle. Separation impulses were obtained from the measurement of the third- and fourth-stage motions and correlated with other ground investigations on the separation mechanism. Visual light scanners and accelerometers were used to obtain a record of the fourth-stage motion, and rate and attitude gyros gave information on the third-stage motion.

The results showed that the impulse during the operation of the separation diaphragm was in good agreement with that measured in ground tests. However, the larger part of the flight-measured impulse occurred immediately following the actual separation of the stages. The total measured impulse was about 5.5 pound-seconds, or more than twice the maximum measured in ground tests. A resulting tipoff angle of 10° was encountered.

The close proximity of the third and fourth stages during and following ignition was concluded to be the main cause of the tipoff impulse.

INTRODUCTION

The guidance of the fourth stage of the Scout vehicle is obtained by pointing this stage in the proper direction while it is still attached to the third stage and spinning it by firing four spin rockets located at the base of fourth stage. The fourth stage is then ignited and separated while spinning, and its original pointing is maintained by the gyroscopic effects. The Scout vehicle is described in reference 1, and a description of the separation system may be found in reference 2.

The efficiency of spin stabilization has been theoretically investigated, and spinning seems to be the most economical method of obtaining attitude stabilization for small rocket motors, where the weight of guidance and control components would offer severe performance penalties. References 3 and 4 discuss methods of analyzing motions of spinning bodies with various disturbances acting.

Reference 2 discusses the results of some of the Scout vehicle flights during which it was apparent that the fourth stage was oriented in a different direction than planned. The study of reference 2 indicated that the change in direction was caused by a disturbance to the spinning vehicle and not an initial pointing error. This investigation was initiated to determine the motion of the spinning stage and from it, an understanding of the forces that produced the motion.

The separation of the third and fourth stages may be understood by referring to figure 1. The volume enclosed by the separation diaphragm and the motor exit nozzle is pressurized by the motor ignition. As the pressure builds up, the diaphragm deflects. The deflection releases the threads around the periphery of the diaphragm and permits the fourth stage to leave the third.

Two horizon scanners mounted on the spinning vehicle provided data from which the pitching motion of the vehicle could be calculated. Accelerometers provided information on the total transverse and normal accelerations of the fourth stage, and radar tracking permitted gross estimates of the vehicle trajectory. In addition, forces acting on the third stage were determined from measured body angular rates during fourth-stage spinup and separation.

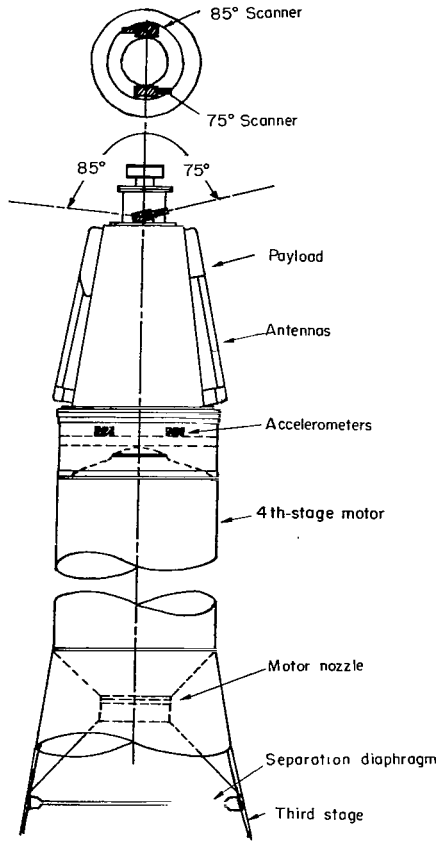

Figure 1.- Schematic diagram of fourth stage showing mounting of scanners and accelerometers.

This report presents the results of the flight of the ST-7 vehicle, in which a large separation disturbance was present, and examines the motions of the third and fourth stages to find the source of the disturbing force.

SYMBOLS

h	altitude of the vehicle, nautical miles
I_x	roll moment of inertia, slug-ft^2
M	disturbing moment, ft-lb
p	spin rate, radians/sec
R	radius of the earth, nautical miles
t	time, sec
X,Y,Z	body-axis system centered at the body center of gravity
X',Y',Z'	earth-axis system centered at the earth's center
α	earth scan-angle correction parameter

β earth scan angle, deg

$\Delta\beta$ scan-angle correction, deg

θ Euler body pitch angle, deg

θ_c pitch plane tipoff angle, deg

θ_o initial body pitch angle above local horizontal, deg

θ_t total body pitch angle above local horizontal, deg

δ scanner mounting angle, deg

ϵ tipoff angle, deg

ψ_c yaw plane tipoff angle, deg

τ time during which a disturbing moment is acting, sec

INSTRUMENTATION

Horizon Scanners

Fixed telescopes having a 1^o circular field of view were mounted on the front end of the spinning vehicle as shown in figure 1. A record of the pitching motions was obtained with these horizon scanners. The sensing elements for the scanners were lead sulphide cells which, with the optics, were sensitive to visible light and the near infrared to about 3 microns. Thus, the scanners responded almost entirely to earth reflected solar radiation.

A sample of the records obtained are reproduced in figure 2. The spinning motion of the vehicle was such that the scan first intercepted the southern horizon and passed from earth to space at the northern horizon. Since the sun was south of the equator at the time of the experiment, the reflected light from the southern horizon produced a high-level signal from the scanner. As the scanner passed over the earth, the reflected light intensity dropped off until the scanner saw space (zero signal) and repeated the cycle. Subsequent to the ignition of the spinning stage, one of the scanners was pointed in the vicinity of the sun, as shown on the records in figure 2 by the steep high peaks between the horizon pulses.

Two horizon scanners were used to cover the possibilities of large changes in body attitude in either the up or down direction. In this flight the vehicle pitched down; had the vehicle pitched up, one of the scanners would not have seen the horizon.

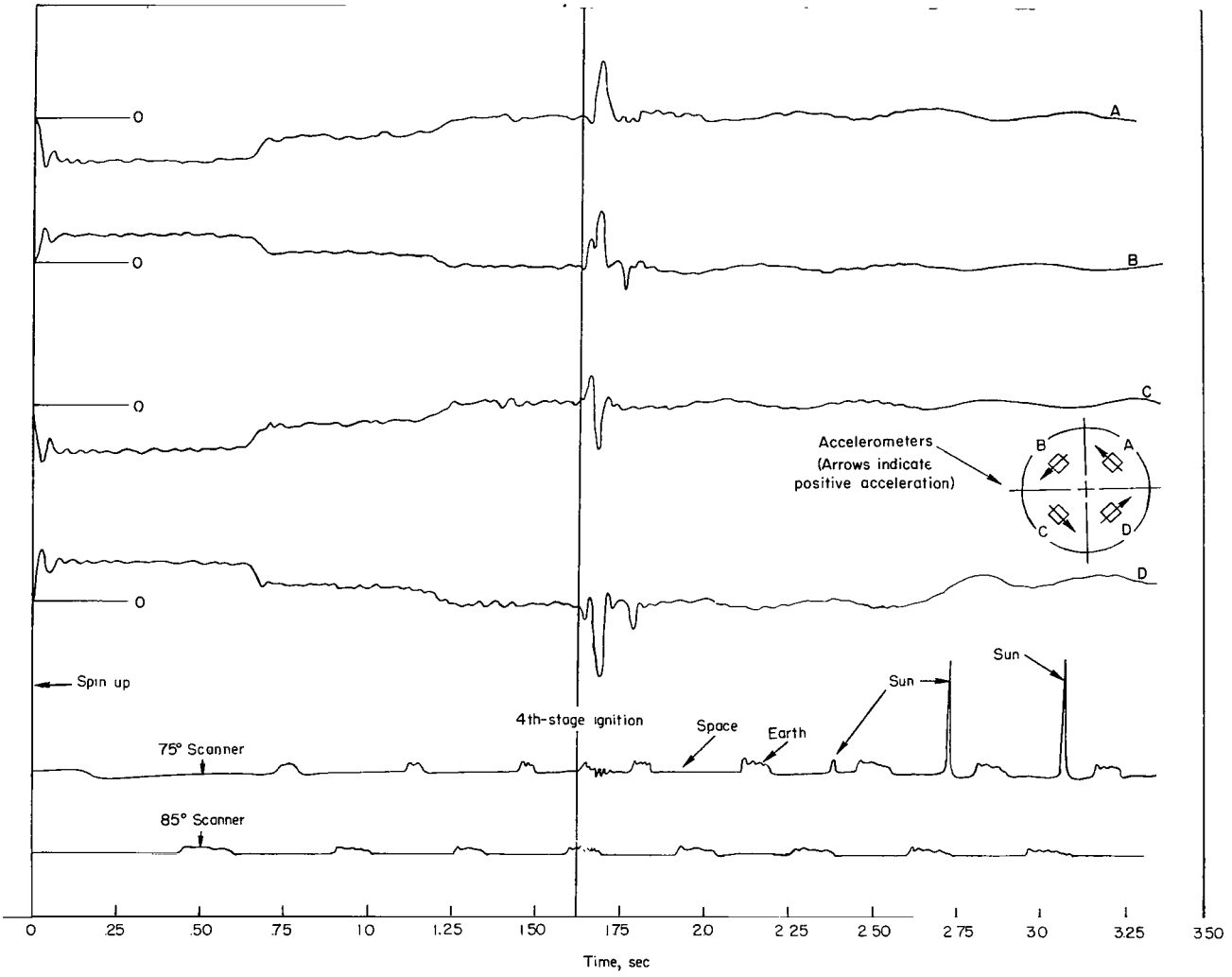

Figure 2.- Time history of scanner and accelerometer outputs.

Accelerometers

The four accelerometers mounted behind the payload in the fourth stage provided a record of the transverse and normal accelerations of the vehicle. It was possible to analyze these data by the method of reference 2 and to obtain the total disturbing impulse; also, from the known configuration of the vehicle, the total orientation error of the spinning stage could be obtained. This orientation error is here defined as tipoff. With a spinning body, it is the precession angle through which the body moves after being disturbed. The nutation frequency was measured directly from the accelerometer records.

Third-Stage Instruments

The data obtained and used from the third stage were the outputs of vehicle guidance-system attitude and rate gyros. These instruments provided angular

rate and position time histories from which moments acting on the third stage could be deduced. The attitude information made it possible to estimate the relative positions of the third and fourth stages during the separation process.

Radar

Radar data included measurements of vehicle altitude, distance, and velocity from which the orientation and magnitude of the velocity vector were determined. Radar information on the third stage was excellent and provided good velocity vector and altitude data at ignition of the fourth stage. Tracking was lost at the time and scant information was obtained on the fourth stage itself. The radar data, because of the lack of fourth-stage information, serve only as a rough check on the final-stage behavior.

DATA ANALYSIS

Roll Rate

The sun pulses, shown in figure 2, obtained on the 75° scanner, provided roll-rate information. The roll rate is proportional to the reciprocal of the time interval between pulses. Since the solar pulses provided sharper, hence more easily read, signals than the earth pulses, they were used whenever they appeared. The time history of roll rate after ignition, as obtained from the sun pulses, is shown in figure 3(a). Figure 3(b) was obtained from the earth scan and shows the roll-rate time history prior to and immediately following ignition of the fourth-stage engine. The earth pulses provided good information for these data since there were no significant disturbances during this period. The sun did not appear in the scan until ignition and oscillation of the fourth stage.

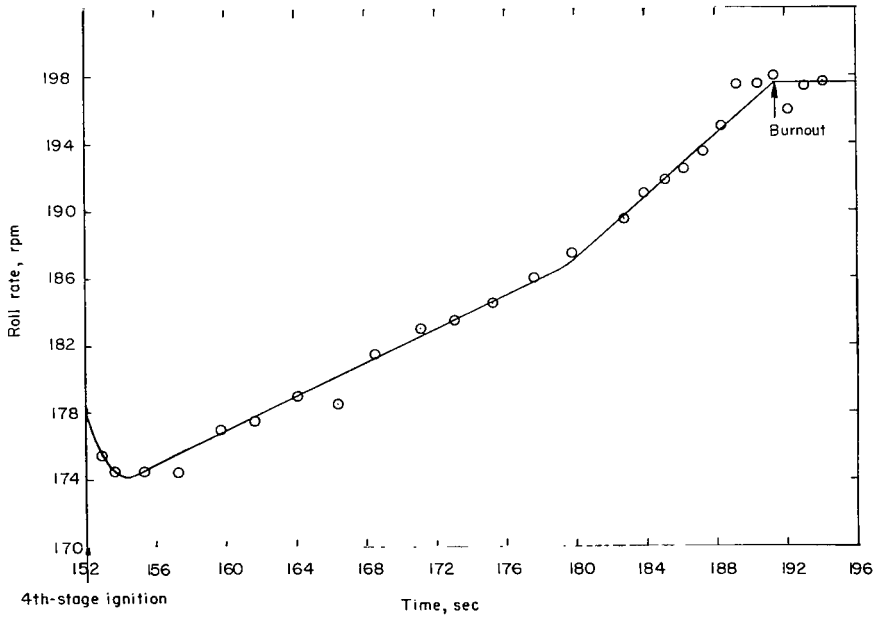

(a) Time history during fourth-stage burning from sun pulses.

Figure 3.- Roll-rate time histories from 75° horizon scanner.

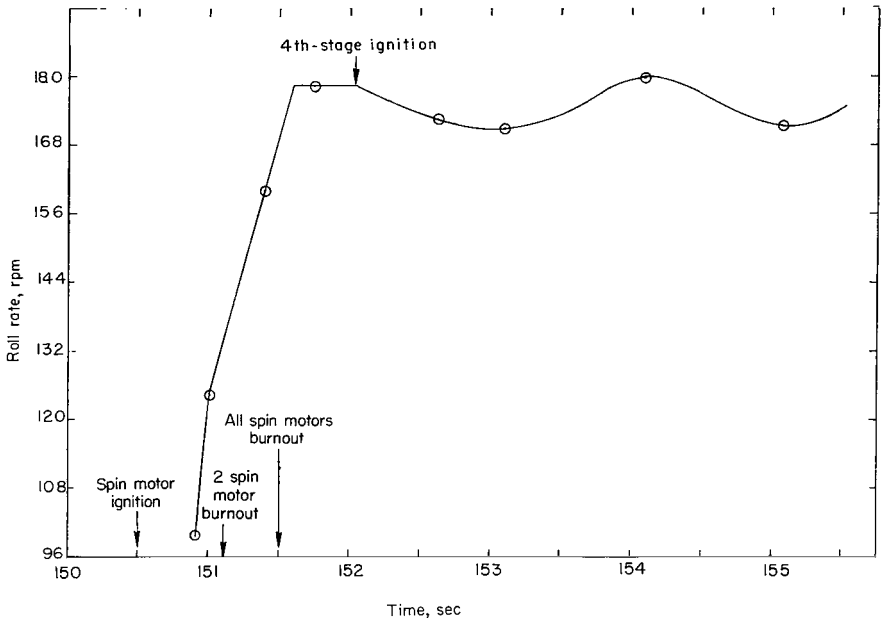

(b) Time history from earth pulses.

Figure 3.- Concluded.

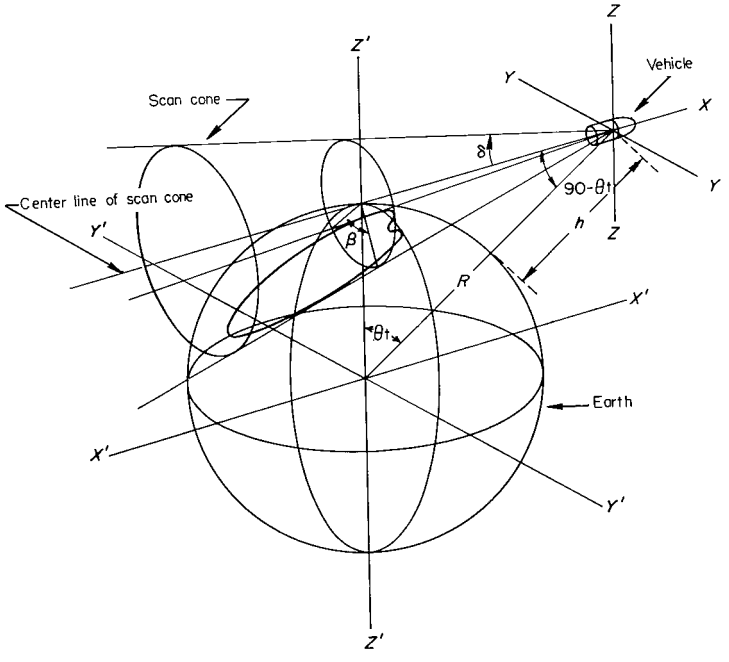

Figure 4.- Geometry of scan.

Pitch Attitude

The scanner telescopes describe a cone in space which intersects with an assumed spherical earth. The geometry of the scan is shown in figure 4. The parameters of the scan are: altitude, portion of the scan which intersects the earth, scan-cone half-angle, body-pitch angle of the vehicle, and radius of the earth. All of these parameters are known from the vehicle design, instrumentation, and radar data except the body-pitch angle. The altitude is obtained from the radar data; the angle during which the scanner sees the earth is obtained from the scan data; and the other parameters such as the inertias and telescope pointing angle relative to the roll reference axis are fixed in the design of the experiment.

The intersection of the scan and earth is mathematically described by the equations presented in the appendix. The equations were solved on a digital computer for the specific configuration of the ST-7 vehicle, and the results are shown in figure 5(a). The angle β was obtained by multiplying the rate of roll by the time of earth scan. The equations of the appendix indicate that the signal output of the scanner begins as soon as the edge, rather than the center line, of the scanner field of view touches the horizon. The resulting difference in measured earth angle is therefore a function of the angle at which the scan actually crosses the horizon. The equations used to determine the correction to β are given in the appendix. Figure 5(b) shows the corrections, calculated for the ST-7 vehicle.

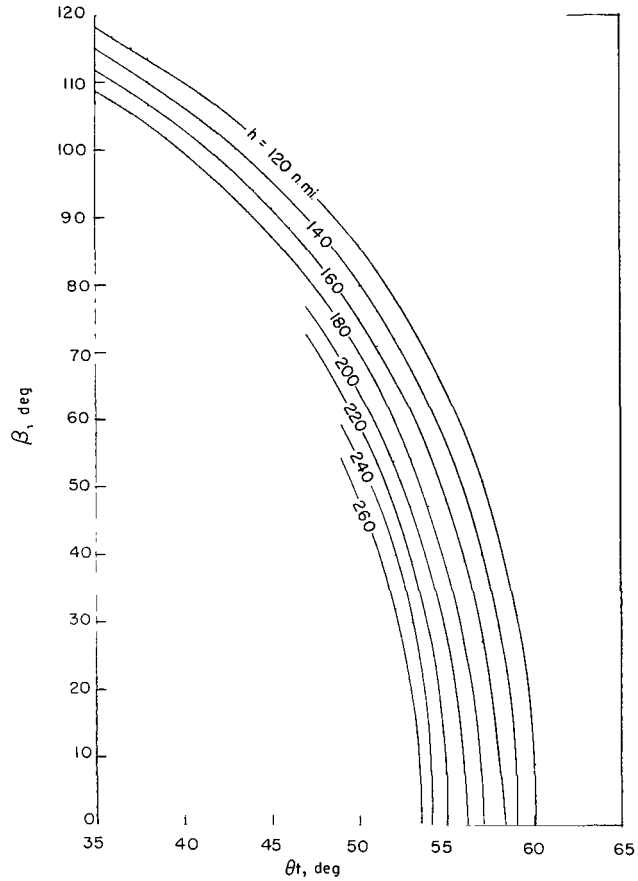

(a) Variation of earth scan angle with altitude and body-pitch angle.

Figure 5.- Curves for solution of scan-geometry equations for 75° scanner.

Because the signal output of the scanner begins to rise when the scanner field of view first encounters the earth's atmosphere and not when it finally crosses the earth's surface, an additional correction to β is necessary. The mean altitude of the fourth stage during burning was about 200 nautical miles. At this altitude the angular difference between the horizon at the earth's surface and at the upper layer of clouds (assumed at an altitude of 5 nautical miles) is about 0.25°. Since the scanner output starts at 0.25° above the horizon when first crossing (and persists for 0.25° after passing) the horizon, a value of 0.50° was subtracted from the scan angle.

The procedure used to determine the time history of the body-pitch angle of the vehicle is as follows:

1. Multiply roll rate by earth pulse width to obtain β.

2. Enter the curves of figure 5(a) with values of β and altitude determined from radar to obtain θ_t.

3. Enter curves of figure 5(b) with θ_t and h to obtain $\Delta\beta$.

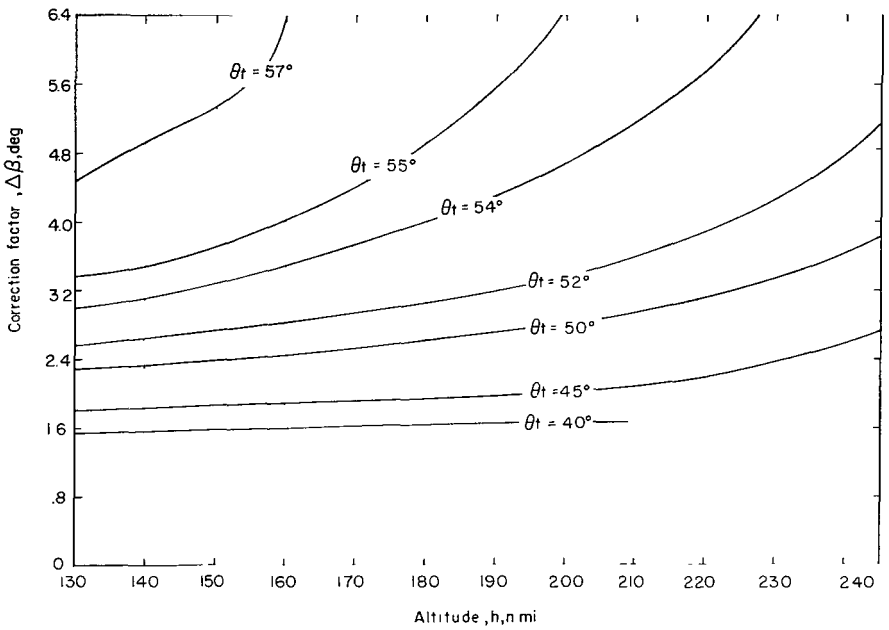

(b) Earth-angle correction factors.

Figure 5.- Concluded.

4. Subtract $\Delta\beta$ from β. Subtract an additional 0.5° from β to account for the height of the earth's atmosphere to obtain the corrected β.

5. Enter the curves of figure 5(a) with the corrected β and h to obtain the corrected θ_t.

The time history of vehicle body-pitch angle is shown in figure 6. The Euler pitch angle θ may be obtained from this information by the relationship

$$\theta = \theta_t - \theta_o$$

$$\theta = \theta_t - 57.2$$

The value used for the initial body-pitch angle is explained subsequently.

Errors in Data and Computations

The roll-rate determination depended on the time interval between either sun or earth pulses. Because of the slope of these pulses and the small distances on the record involved, the best time accuracy is about 2.0 milliseconds out of approximately 335 milliseconds per revolution. The resulting error in roll rate is about 1.1 rpm.

The pitch-attitude errors are also an important function of the accuracy with which the time can be read during the earth scan. This time error is considered to be about 2 milliseconds. The rolling velocity error, because it contributes to the earth scan angle, is also important. An additional error, based on estimates of the reliability of the radar information, lies in the altitude. This error was assumed to be about ±2.0 nautical miles. Another altitude error exists in that the altitude is increasing during the earth scan. Calculations show that the altitude rate will cause a maximum error in θ_t of about -0.2°.

It can be seen from the curves of figure 5(a) that the relationship between the angles β and θ_t and the altitude h are such that the values obtained for θ_t become more uncertain as θ_t is reduced. Thus, the error in θ_t resulting from errors in β and h is an important function of θ_t itself.

The noise in the telemetered signals was of such magnitude as to cause some error in reading the earth pulse width. Since the noise was not consistent, the error contributed by it varied from point to point.

The errors from all the sources were considered and applied to various calculated points during the data-reduction procedure. The results are shown in figure 6 on the pitch time history. Generally, when the vehicle pitched down to low angles, the errors were significantly larger. Errors of about $\pm 0.4^{\circ}$ in θ_t were obtained at high values of θ_t, whereas errors as high as $\pm 3.0^{\circ}$ were possible at very low values. These errors were obtained by using the highest cumulative total from the error sources. The small rate of change of signal amplitude with time evident on the 85° scanner (as shown in fig. 2) produced large errors in time readings for that scanner. These errors rendered the data from the 85° scanner relatively unreliable. These data were consequently not used except for general verification of the data from the 75° scanner. The main reason for incorporating the 85° scanner in the system was to cover the possibility of a tip-up rather than a tip-down attitude change. Had this change occurred, the 75° scanner may not have intersected the horizon.

RESULTS

Scanner Data

The scanners mounted in the spinning fourth stage provided the information for the time history of the pitch-attitude angle in figure 6. These scanners provided pitch-attitude information prior to ignition of the final stage. The plotted points show that the vehicle pitch angle resulting from the guidance program of the Scout vehicle was $57.2^{\circ} \pm 0.4^{\circ}$. The predicted angle at this

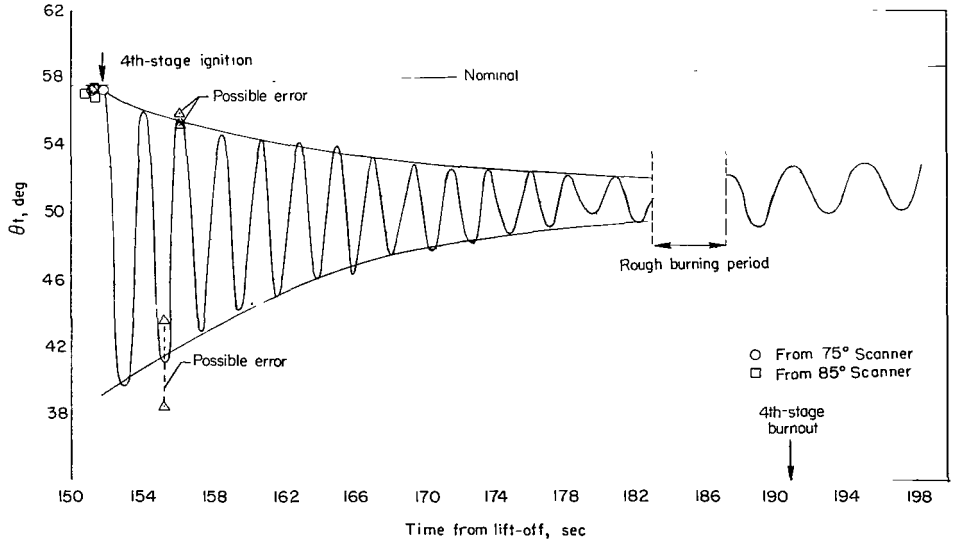

Figure 6.- Time history of fourth-stage motion in pitch plane.

time was $57.6^\circ \pm 0.5^\circ$. After ignition, a coning or precession of the fourth stage was produced, in addition to the nutation of the spinning stage due to thrust misalinement. The estimated nutation amplitude was calculated to be about 0.2°, too small for the time history to detect. The center of the coning envelope, the pitch tipoff angle, immediately following ignition of the fourth stage was about 9.1° below the pointing angle prior to ignition.

The pitch motion is marked by an apparent unsymmetrical damping envelope. The result of the jet damping and other forces operating during burning was to reduce the coning from about 18° to 3° and raise the center of the cone from 9.1° pitch-down at ignition to 7.0° pitch-down at burnout. An increase of the nominal angle of 1.2° during burning is shown in figure 6. This change in angle occurs because the vehicle maintains its inertial position while traveling over the spherical earth. The change in angle reflects the change in the local earth vertical.

Calculations, based on the analysis of reference 2, were made, of the total impulse disturbance required to produce the motion encountered. The equations for the tipoff angles in the pitch and yaw planes for a body-fixed moment are

$$\left.\begin{aligned} \theta_c &= \frac{M}{I_x p^2} \sin(p\tau) \\ \psi_c &= \frac{M}{I_x p^2}\left[\cos(p\tau) - 1\right] \end{aligned}\right\} \tag{1}$$

The total tipoff angle is then

$$\epsilon = \frac{2M}{I_x p^2} \sin \frac{p\tau}{2} \tag{2}$$

Taking the ratio of pitch angle to total tipoff gives

$$\cos(p\tau) = 2\left(\frac{\theta_c}{\epsilon}\right)^2 - 1 \tag{3}$$

and solving for M from equation (2) yields

$$M = \frac{\epsilon I_x p^2}{2 \sin \frac{p\tau}{2}} \tag{4}$$

Equations (3) and (4) were plotted against equation (2) in figure 7 for the case investigated where the pitch tipoff angle of 9.1° was encountered. The data from the fourth-stage accelerometers, which showed a total ϵ of 10°, may be used to enter the curves of figure 7, from which a moment and time are obtained, the product of which is an angular impulse. This is the impulse required to produce the motion observed. An angular impulse of about

20 ft-lb-sec is obtained. With the distance from the fourth-stage center of gravity to the exit plane of the motor of 3.33 ft, the linear impulse is about 6.0 lb-sec. This value is the impulse that would be required if the moment were rotating with the body and applied about the yaw axis.

The roll-rate time history of figure 3 shows an immediate reduction in roll rate following ignition of the engine. After this reduction occurred, the roll rate increased steadily up to a point near the end of burning; then the rate of change increased until burnout, when roll rate reached a steady level.

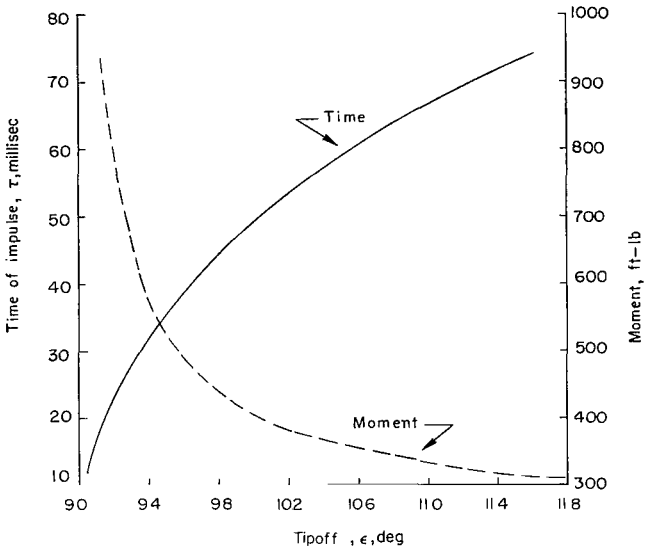

Figure 7.- Disturbing moment and time of disturbance to produce total tipoff for a 9.1° pitch tipoff.

The calculated steady-state moment to provide the required average increase in roll rate for the first increase was about 0.27 ft-lb if the inertia is assumed to vary linearly. The more rapid rate of increase near the end of burning required an average moment of 0.31 ft-lb. These numbers represent averages, and the actual instantaneous moments could be expected to be much larger.

Accelerometer Data

The physical characteristics of the third and fourth stages of the ST-7 Scout vehicle necessary for reduction of the data are given in the following table:

Center-of-gravity station of fourth stage, in.	64
Center-of-gravity station of third stage, in.	164
Center-of-gravity station of attached third and fourth stages, in.	118
Fourth-stage nozzle-exit-plane station, in.	104
Roll inertia of fourth stage, slug-ft^2	5.74
Pitch and yaw inertia of fourth stage, slug-ft^2	39.2
Pitch and yaw inertia of third stage, slug-ft^2	403
Pitch and yaw inertia of attached third and fourth stages, slug-ft^2	1165
Weight of fourth stage, lb	627
Weight of third stage, lb	721

The accelerometer data shown in figure 2 were analyzed by the method of reference 2. The resulting total angular impulse was 18.15 ft-lb-sec or a linear impulse of 5.45 lb-sec applied at the motor exit plane. The impulse corresponded to a total initial body pitching rate of 26.6° per second and resultant tipoff angle of 10°. These values are based on the assumption that an

impulsive disturbing moment was applied at separation of the spinning fourth stage. The total impulse, resolved into an average moment operating for a short period of time, produces the body rate and tipoff angle calculated. It should also be noted that the maximum peaks on the accelerometer recordings occurred at about 70 to 80 milliseconds after ignition and that the disturbances continued for about 180 milliseconds. The arrows on the accelerometers in figure 2 indicate the direction for positive acceleration measurement. For example, the high peaks on traces A and C indicate that a force on the corresponding accelerometers is applied in the upper left-hand direction.

Third-Stage Angular Rates

The third-stage angular rates are shown in figure 8(a). The time period considered is immediately before the ignition of the fourth stage and for 200 milliseconds following ignition. The time of ignition was taken as the point of the first reading on the transverse accelerometers.

The roll rate shows a large transient immediately following ignition indicating a very large roll disturbance. This large disturbance initiated a corrective torque by the roll-control jets on the third stage. The third-stage pitch and yaw jets did not operate during the time of and immediately following separation. The disturbances shown were due to the separation processes.

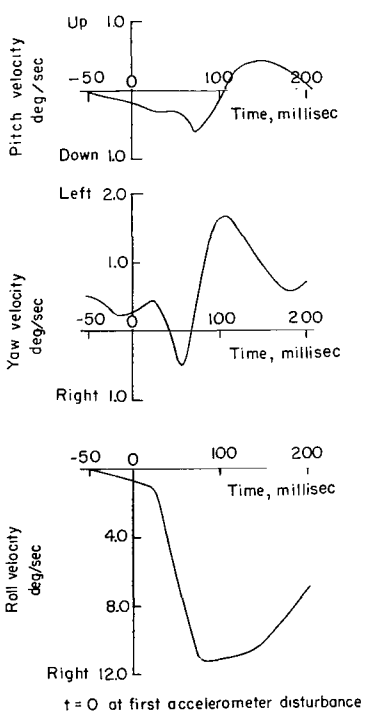

(a) Third-stage angular velocities.

Figure 8.- Third-stage behavior during fourth-stage ignition.

At about 60 milliseconds a reversal in force is evident in the yaw plane and a force is applied in the pitch plane. At about 70 milliseconds there is also a change in the roll moment. The time scale is affected by the telemeter and instrument lags, and the times of rapidly changing events may be in error by as much as 10 milliseconds. If it is assumed that the physical separation of the third and fourth stages occurs at about the time of these discontinuities, then separation occurred at between 60 and 70 milliseconds. Up to this time the impulse derived from these curves is in the proper direction to produce the resulting fourth-stage motion. The total transverse impulse is about 1.7 lb-sec with about 1.6 lb-sec in the pitch plane. This separation impulse and duration is of the same order of magnitude as those measured during ground tests on the fourth-stage motor in reference 5. An additional impulse in the opposite direction was evident from these records after physical separation.

Third-Stage Angular Positions

The third-stage angular positions are shown in figure 8(b) for the same time interval covered by the rate data. The yaw attitude is marked by an apparent

loss of signal during a large part of the interval covered. An assumed time history is shown for this period. The yaw attitude signal was transmitted on a channel that was shared by other data. For this reason, the data were not continuous. The pitch attitude is not zero at this time, but for the purposes of obtaining the relative positions of the third and fourth stages, this is not important. These data are discussed subsequently in describing the vehicle motions.

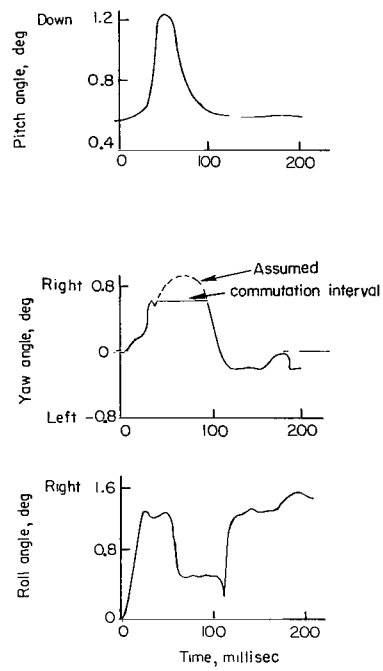

(b) Third-stage attitude angles.

Figure 8.- Concluded.

DISCUSSION OF RESULTS

The results of the analysis of the third-stage motions indicate that a total impulse of about 1.7 lb-sec was applied to the fourth stage after the start of ignition and during the operation of the separation diaphragm. Immediately after diaphragm separation the forces evident on the third stage are acting in the wrong direction to produce the measured fourth-stage motions. The impulse during separation is in good agreement with the data in reference 5 which shows separation impulses from 1.0 to 2.3 lb-sec. However, this impulse is very much lower than the total deduced from the fourth-stage scanner data (6.0 lb-sec) and accelerometers (5.45 lb-sec).

The fourth-stage accelerometers showed disturbances from ignition until about 180 milliseconds later. Calculations show that at this time the separation of the stages is approximately 14 to 16 inches. It will be noted in reference 5 that this time interval corresponds to the approximate time at which the motor chamber pressure has reached its steady-state value. Calculations show that at about 3 to 5 milliseconds after separation, the flow in the nozzle throat becomes sonic.

The sequence of the separation events appears to occur in approximately the times and manner indicated in the following paragraphs. The times are those taken from unpublished data obtained during the ground tests reported in reference 5. These times appear to be in good agreement with the flight measurements. The sequence is schematically illustrated in figure 9.

(1) At $t = 0$ the igniter is actuated.

(2) At $t \approx 30$ milliseconds, the nozzle closure plug is blown and the diaphragm begins deflecting.

(3) At $t \approx 60$ to 70 milliseconds, the stages are physically separated. At this time approximately 20 percent of the total disturbing impulse has been imparted to the fourth stage, and the exhaust gas flow in the nozzle throat becomes sonic.

(4) At $t \approx 70$ to 80 milliseconds, the peak disturbing moment is reached, and the stages are separated about 1/2 inch. The angle between the stages is about 0.25° in pitch and 1.5° in yaw.

(5) At $t \approx 180$ milliseconds, the large disturbing impulses end; the stages have about 14 to 16 inches of separation; precession has started with the relative angles between the stages about 5° in pitch and 1.5° in yaw; the motor chamber pressure has reached a steady-state value.

Two possible sources are responsible for the large impulse experienced. The first is a disturbed flow in the motor itself, while the chamber pressure is undergoing large variations. The investigation of reference 5 failed to reveal any such large impulses for the motor itself; however, the pressure source used in that study was a point instead of the actual burning grain and the difference between the two may be significant.

A second possible cause of the large disturbance is the dynamic interaction of the exhaust gas between the third and fourth stages. The tests of reference 5 used a simulated third stage, wherein not only the mass but also the geometry of the interface was simulated. However, the pitch inertia was considerably smaller because of the space limitations. It is possible that this simulation, while providing the proper separation rate between stages for no transverse force, may have greatly overestimated the separation rate due to rotation of the third stage. The stages would have been in close proximity for a longer time in the actual flight than in the simulation and thus would tend to produce greater interaction and higher impulses. It is also possible that body-spin has a significant effect. Spin was not investigated in the ground tests. The transverse disturbance due to the close proximity of the stages may be described with reference to figure 9. The pitch and yaw attitudes of the third stage were obtained from the telemetered record of the guidance-system gyro reference. These records are shown in figure 8(b). The attitudes of the fourth stage are very approximate and are deduced from calculations based on the

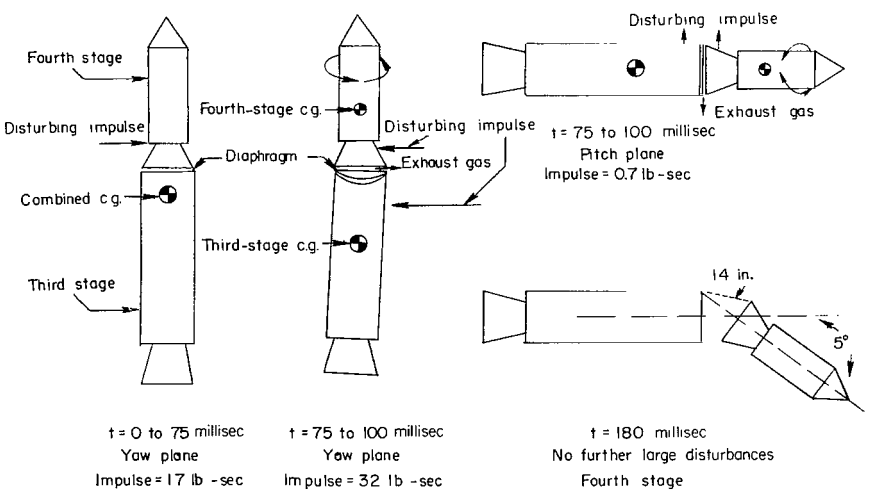

Figure 9.- Third- and fourth-stage relative positions during separation.

moments obtained from figure 7. The separation between stages was calculated from an assumed thrust time history based on the results of reference 5. The impulses obtained are those derived from the change in angular rates of the third stage.

The impulse and forces in the assumed sequence are all in the proper directions and roughly of the correct magnitude to produce the motions measured. Although the calculations and sequence are only approximate, it is believed that they represent a reasonable estimate of the situation. A more detailed study of the motions would increase the complexity of the analysis beyond the scope of this paper. It would require data which are not available, and the necessary assumptions would make its accuracy questionable.

CONCLUSIONS

An investigation of the tipoff of the final stage of the Scout vehicle was conducted during a flight in which a large disturbance was detected. The following conclusions were reached:

1. A tipoff disturbance of about 5.5 to 6.0 lb-sec was produced, and it caused a total tipoff angle of 10°. The tipoff in the pitch plane was 9.1° pitch-down.

2. The separation disturbance, estimated from third-stage instrumentation during the time of separation, was about 1.7 lb-sec. The magnitude of this impulse is in agreement with ground investigations.

3. The largest impulse was obtained after separation and lasted until a separation distance of 14 to 16 inches was reached. This disturbance was believed due to the close proximity of the stages and the interaction of exhaust gases during this time.

4. The use of the separation diaphragm provided the possibility of a large tipoff because of the possibility of its unsymmetrical release and its requirement for the close proximity of the stages during ignition.

5. An average roll moment of about 0.3 foot-pound during fourth-stage burning was measured.

6. The third-stage pitch angle at ignition of the fourth stage was within the guidance system tolerances.

7. Visible radiation horizon scanners were satisfactorily used to produce a time history of body-attitude angle during fourth-stage operation.

Langley Research Center,
National Aeronautics and Space Administration,
Langley Station, Hampton, Va., September 14, 1964.

APPENDIX

THE GEOMETRICAL RELATIONSHIPS OF THE EARTH SCANNER AND SPACE VEHICLE

The use of the horizon scanners in the experiment was based on an unpublished analysis of the geometrical relationships of the vehicle in space in the vicinity of the earth. The analysis was performed by Mr. J. W. Youngblood of the Langley Research Center. The geometry problem is illustrated in figure 4. The analysis resulted in the following applicable simultaneous equations:

$$\cos \beta = \frac{2\left[\left(2Rh + h^2\right)^{1/2} - (R + h)\cos \delta \sin \theta\right]^2}{(R + h)^2 \sin \delta \cos^2 \theta} - 1 \tag{A1}$$

$$\sin \theta = \frac{2\left(2Rh + h^2\right)^{1/2} \cos \delta \pm \sin \delta \sqrt{2R^2(1 + \cos \beta) - (R + h)^2 \sin^2 \delta \sin^2 \beta}}{(R + h)\left[\sin^2 \delta (1 + \cos \beta) + 2 \cos^2 \delta\right]} \tag{A2}$$

These equations were solved simultaneously on a digital computer for the earth scan angle β and the body-pitch angle θ. A range of values of altitude was selected to cover the altitude range for which the attitude information was desired. The scanner mounting angle δ was determined and was also used as an independent variable in the equations. The results of the computer solutions are plotted in figure 5(a).

Mr. Youngblood's analysis took into account the fact that the scan was of finite dimensions and not a simple line. The finite scan crosses the horizon before its center line, and the result is that the apparent earth scan angle β is larger than the true angle. The correction equations developed by Mr. Youngblood are:

$$\Delta\beta = \csc \alpha \tag{A3}$$

$$\cos \alpha = \left(\frac{R + h}{R}\right)\frac{\sin \theta}{\sin \delta} - \frac{\left(2Rh + h^2\right)^{1/2}}{R} \cot \delta \tag{A4}$$

The correction factor $\Delta\beta$ was calculated for a range of altitudes and body angles to cover the actual flight ranges of these parameters. The correction factor is plotted in figure 5(b).

REFERENCES

1. Mayhue, Robert J., compiler: NASA Scout ST-1 Flight-Test Results and Analyses, Launch Operations, and Test Vehicle Description. NASA TN D-1240, 1962.

2. Young, George R.; and Buglia, James J.: An Analysis of the Coning Motions of the Final Stages of Three NASA Scout Development Vehicles. NASA TN D-1396, 1962.

3. Suddath, Jerrold H.: A Theoretical Study of the Angular Motions of Spinning Bodies in Space. NASA TR R-83, 1961.

4. Buglia, James J.; Young, George R.; Timmons, Jesse D.; and Brinkworth, Helen S.: Analytical Method of Approximating the Motion of a Spinning Vehicle With Variable Mass and Inertia Properties Acted Upon by Several Disturbing Parameters. NASA TR R-110, 1961.

5. Gungle, Robert L.; Brosier, William S.; and Leonard, H. Wayne: An Experimental Technique for the Investigation of Tipoff Forces Associated With Stage Separation of Multistage Rocket Vehicles. NASA TN D-1030, 1962.

NASA-Langley, 1965 L-3175

"The aeronautical and space activities of the United States shall be conducted so as to contribute . . . to the expansion of human knowledge of phenomena in the atmosphere and space. The Administration shall provide for the widest practicable and appropriate dissemination of information concerning its activities and the results thereof."

—NATIONAL AERONAUTICS AND SPACE ACT OF 1958

NASA SCIENTIFIC AND TECHNICAL PUBLICATIONS

TECHNICAL REPORTS: Scientific and technical information considered important, complete, and a lasting contribution to existing knowledge.

TECHNICAL NOTES: Information less broad in scope but nevertheless of importance as a contribution to existing knowledge.

TECHNICAL MEMORANDUMS: Information receiving limited distribution because of preliminary data, security classification, or other reasons.

CONTRACTOR REPORTS: Technical information generated in connection with a NASA contract or grant and released under NASA auspices.

TECHNICAL TRANSLATIONS: Information published in a foreign language considered to merit NASA distribution in English.

TECHNICAL REPRINTS: Information derived from NASA activities and initially published in the form of journal articles.

SPECIAL PUBLICATIONS: Information derived from or of value to NASA activities but not necessarily reporting the results of individual NASA-programmed scientific efforts. Publications include conference proceedings, monographs, data compilations, handbooks, sourcebooks, and special bibliographies.

Details on the availability of these publications may be obtained from:

SCIENTIFIC AND TECHNICAL INFORMATION DIVISION

NATIONAL AERONAUTICS AND SPACE ADMINISTRATION

Washington, D.C. 20546